KAPLAN & SADOCK'S COMPREHENSIVE TEXTBOOK OF PSYCHIATRY

NINTH EDITION

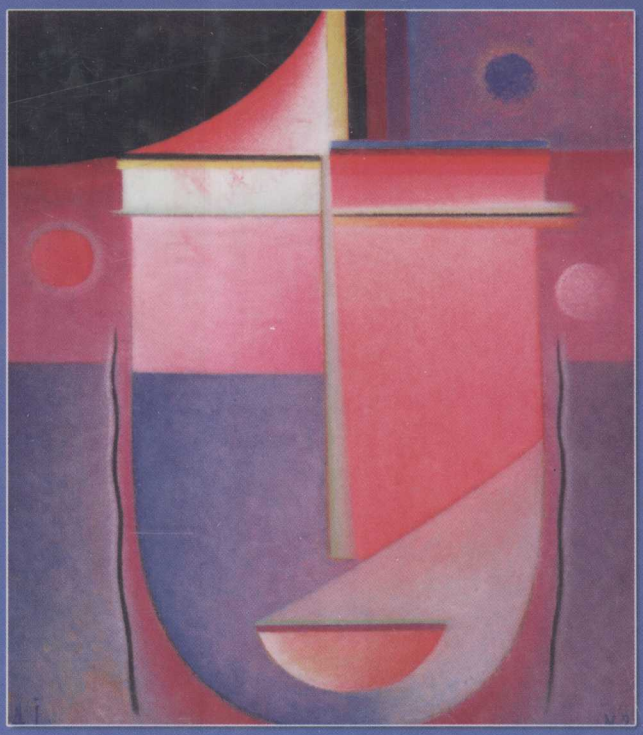

EDITORS

BENJAMIN JAMES SADOCK, M.D.
VIRGINIA ALCOTT SADOCK, M.D.
PEDRO RUIZ, M.D.

Includes online fully searchable text. Details inside!

Wolters Kluwer Health | Lippincott Williams & Wilkins

VOLUME I

KAPLAN & SADOCK'S

COMPREHENSIVE TEXTBOOK OF PSYCHIATRY

VOLUME I

NINTH EDITION

EDITORS

Benjamin J. Sadock, M.D.

Menas S. Gregory Professor of Psychiatry, Department of Psychiatry,
New York University School of Medicine, NYU Langone Medical Center
Attending Psychiatrist, Tisch Hospital
Attending Psychiatrist, Bellevue Hospital Center
Honorary Medical Staff, Department of Psychiatry, Lenox Hill Hospital
New York, New York

Virginia A. Sadock, M.D.

Professor of Psychiatry,
New York University School of Medicine, NYU Langone Medical Center
Attending Psychiatrist, Bellevue Hospital Center
New York, New York

Pedro Ruiz, M.D.

Professor and Interim Chair, Department of Psychiatry and Behavioral Sciences,
University of Texas Medical School at Houston
Houston, Texas

Wolters Kluwer Health | Lippincott Williams & Wilkins

Philadelphia • Baltimore • New York • London
Buenos Aires • Hong Kong • Sydney • Tokyo

Acquisitions Editor: Charles W. Mitchell
Managing Editor: Sirkka E. Howes
Marketing Manager: Kimberly Schonberger
Production Manager: Bridgett Dougherty
Senior Manufacturing Manager: Benjamin Rivera
Design Coordinator: Stephen Druding
Compositor: Aptara®, Inc.

530 Walnut Street
Philadelphia, PA 19106 USA
LWW.com

Printed in the USA

Library of Congress Cataloging-in-Publication Data

Kaplan & Sadock's comprehensive textbook of psychiatry / [edited by]
Benjamin James Sadock, Virginia Alcott Sadock, Pedro Ruiz. – 9th ed.
p. ; cm.
Includes bibliographical references and index.
ISBN-13: 978-0-7817-6899-3 (alk. paper)
ISBN-10: 0-7817-6899-3 (alk. paper)
1. Psychiatry—Textbooks. I. Sadock, Benjamin J. II. Sadock, Virginia A.
III. Ruiz, Pedro IV. Kaplan, Harold I., 1927–1998 V. Title: Kaplan and Sadock's
comprehensive textbook of psychiatry. VI. Title: Comprehensive textbook of psychiatry.
[DNLM: 1. Mental Disorders. 2. Psychiatry. WM 100 K173 2009]
RC454.C637 2009
616.89—dc22

2009011007

To purchase additional copies of this book, call our customer service department at (800) 638-3030 or fax orders to (301) 223-2320. International customers should call (301)223-2300.

Visit Lippincott Williams & Wilkins on the Internet: at LWW.com. Lippincott Williams & Wilkins customer service representatives are available from 8:30 am to 6 pm, EST.

Cover Illustration: *Looking Within: Rosy Light* by Alexi von Jawlensky (1864-1941).
Used with permission, Artists Right Society (ARS) New York

10 9 8 7 6 5 4 3 2 1

Drugs Used in Psychiatry

This guide contains color reproductions of some commonly prescribed psychotherapeutic drugs. This guide mainly illustrates proprietary tablets and capsules. A † preceding the name of a drug indicates that other doses are available. Check directly with the manufacturer. (*Although the photos are intended as accurate reproductions of the drug, this guide should be used only as a quick identification aid.*)

†ABILIFY®

10 mg 15 mg

aripiprazole
Bristol-Myers Squibb

†ADDERALL XR®

10 mg

dextroamphetamine saccharate, dextroamphetamine sulfate, amphetamine aspartate, amphetamine sulfate
Shire US Inc.

AMBIEN®

5 mg 10 mg

zolpidem tartrate
Searle

ANAFRANIL®

25 mg

clomipramine HCl
Basel

ANTABUSE®

250 mg 500 mg

disulfiram
Odyssey Pharmaceuticals

ASENDIN®

25 mg 50 mg

100 mg 150 mg

amoxapine
Lederle

†ATARAX®

10 mg 25 mg

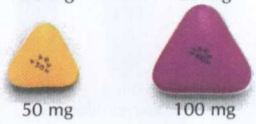

50 mg 100 mg

hydroxyzine HCl
Roerig

ATIVAN®

0.5 mg

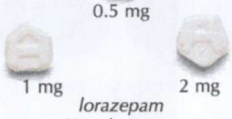

1 mg 2 mg

lorazepam
Wyeth-Ayerst

BUSPAR®

5 mg 10 mg

buspirone HCl
Bristol-Myers Squibb

†CLOZARIL®

100 mg

clozapine
Sandoz

†COGENTIN®

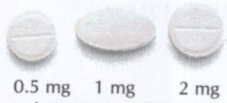

0.5 mg 1 mg 2 mg

benztropine mesylate
Merck & Co.

†COGNEX®

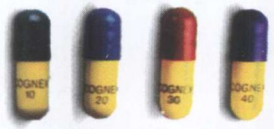

10 mg 20 mg 30 mg 40 mg

tacrine HCl
Parke-Davis

†COMPAZINE®

5 mg 10 mg 25 mg

prochlorperazine
SmithKline Beecham

†COMPAZINE® SPANSULE®

10 mg

15 mg

prochlorperazine
SmithKline Beecham

CYLERT®

18.75 mg

pemoline
Abbott

DALMANE®

15 mg

30 mg

flurazepam HCl
Roche

DEPAKENE®

250 mg

valproic acid
Abbott

DEPAKOTE®

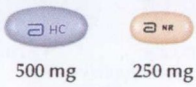

500 mg 250 mg

125 mg sprinkle

divalproex sodium
Abbott

†DEPAKOTE ER®

500 mg

divalproex sodium
Abbott

DESYREL®

50 mg 100 mg

trazodone HCl
Apothecon

†DESYREL® DIVIDOSE®

150 mg

trazodone HCl
Apothecon

† DEXEDRINE®

5 mg

dextroamphetamine
SmithKline Beecham

DORAL®

7.5 mg 15 mg

quazepam
Wallace Laboratories

†EFFEXOR®

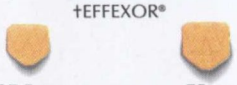

37.5 mg 75 mg

venlafaxine HCl
Wyeth-Ayerst

†ELAVIL®

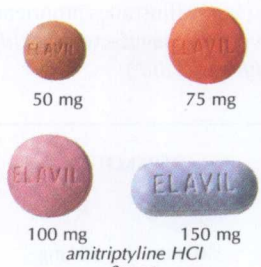

50 mg 75 mg

100 mg 150 mg

amitriptyline HCl
Stuart

†ELDEPRYL®

5 mg
selegiline HCl
Somerset Pharmaceuticals

†ENDEP®

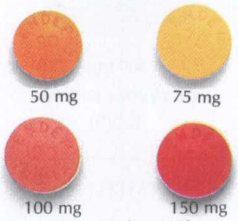

50 mg 75 mg

100 mg 150 mg

amitriptyline HCl
Roche

†ESKALITH®

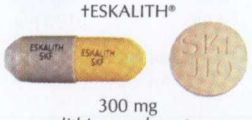

300 mg
lithium carbonate
SmithKline Beecham

GEODON®

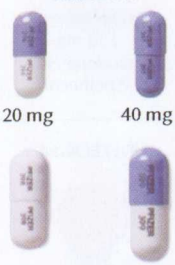

20 mg 40 mg

60 mg 80 mg

ziprasidone
Pfizer

HALCION®

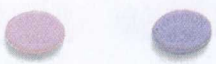

0.125 mg 0.25 mg

triazolam
Upjohn

HALDOL®

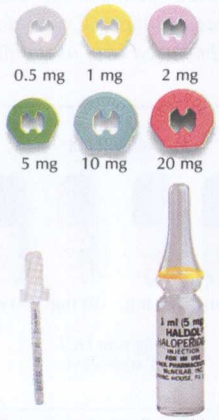

0.5 mg 1 mg 2 mg

5 mg 10 mg 20 mg

Concentrate
2 mg per mL

Injectable
5 mg/mL
(1 mL/ampul)

haloperidol
McNeil Pharmaceutical

†HALDOL® Decanoate

1 mL ampul
haloperidol
McNeil Pharmaceutical

KEMADRIN®

5 mg
procyclidine HCl
Burroughs Wellcome

KLONOPIN®

0.5 mg 1 mg 2 mg
clonazepam
Roche

†LAMICTAL®

25 mg 100 mg
lamotrigine
Glaxo Wellcome

LARODOPA®

0.1 g 0.25 g 0.5 g
levodopa
Roche

†LEXAPRO®

10 mg
escitalopram oxalate
Forest

†LIBRIUM®

5 mg 10 mg 25 mg
chlordiazepoxide HCl
Roche

†LOXITANE®

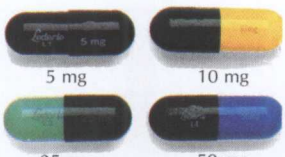

5 mg 10 mg

25 mg 50 mg
loxapine succinate
Lederle

LUDIOMIL®

25 mg 50 mg 75 mg
maprotiline HCl
Novartis

LUVOX®

50 mg 100 mg
fluvoxamine maleate
Solvay

MARPLAN®

10 mg
isocarboxazid
Roche
(no longer manufactured)

†MELLARIL®

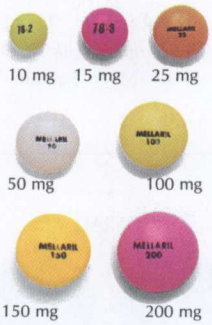

10 mg 15 mg 25 mg

50 mg 100 mg

150 mg 200 mg

thioridazine
Sandoz

METHADONE HCl DISKET®

Eli Lilly

†MOBAN®

50 mg
molindone HCl
Du Pont Multi-Source Products

†NAMENDA®

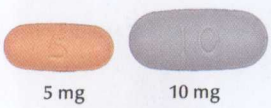

5 mg 10 mg

memantine HCl
Forest

NARDIL®

15 mg
phenelzine sulfate
Parke-Davis

LIPPINCOTT WILLIAMS & WILKINS©

†NAVANE®

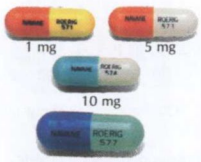

1 mg 5 mg 10 mg 20 mg

thiothixene
Roerig

†NEMBUTAL®

100 mg

pentobarbital sodium
Abbott

†NORPRAMIN®

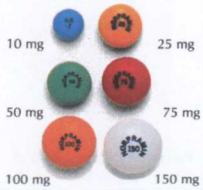

10 mg 25 mg 50 mg 75 mg 100 mg 150 mg

desipramine HCl
Marion Merrell Dow

†ORAP®

2 mg

pimozide
Gate

†PAMELOR®

10 mg 25 mg 50 mg 75 mg

nortriptyline HCl
Sandoz

†PARLODEL®

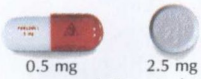

0.5 mg 2.5 mg

bromocriptine mesylate
Sandoz

PARNATE®

10 mg

tranylcypromine sulfate
SmithKline Beecham

PAXIL®

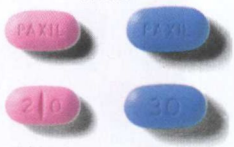

20 mg 30 mg

paroxetine HCl
SmithKline Beecham

†PAXIL CR®

12.5 mg 25 mg

paroxetine HCL
GlaxoSmithKline

†PERMITIL®

10 mg

fluphenazine HCl
Schering/White

†PLACIDYL®

750 mg

ethchlorvynol
Abbott

PONDIMIN®

20 mg

fenfluramine HCl
A.H. Robins
(no longer manufactured)

†PRISTIQ®

50 mg

desvenlafaxine
Wyeth Pharmaceuticals Inc.

†PROLIXIN®

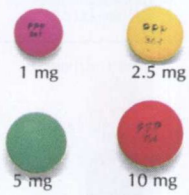

1 mg 2.5 mg 5 mg 10 mg

fluphenazine HCl
Apothecon

†PROSOM®

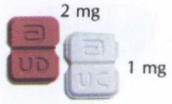

2 mg 1 mg

estazolam
Abbott

†PROVIGIL®

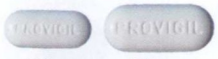

100 mg 200 mg

modafinil
Cephalon

PROZAC®

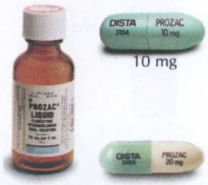

10 mg 20 mg/5 mL 20 mg

90 mg (extended release)

fluoxetine HCl
Dista

REMERON®

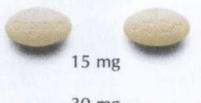

15 mg 30 mg

mirtazapine
Organon

RESTORIL®

15 mg 30 mg

temazepam
Sandoz

REVIA®

50 mg

naltrexone HCl
DuPont

†RISPERDAL®

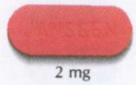

2 mg

risperidone
Janssen

RITALIN®

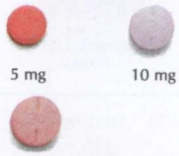

5 mg 10 mg 20 mg

methylphenidate HCl
Novartis

†SERAX®

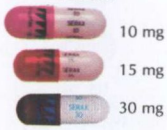

10 mg 15 mg 30 mg

oxazepam
Wyeth-Ayerst

†SERENTIL®

10 mg

mesoridazine besylate
Boehringer Ingelheim

†SEROQUEL®

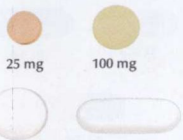

25 mg 100 mg 200 mg 300 mg

quetiapine fumarate
AstraZeneca

SINEMET®

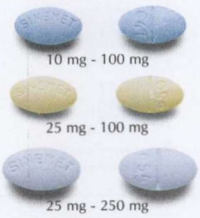

10 mg - 100 mg 25 mg - 100 mg 25 mg - 250 mg

carbidopa-levodopa
DuPont

SINEMET® CR

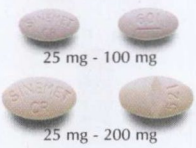

25 mg - 100 mg 25 mg - 200 mg

carbidopa-levodopa
sustained release
DuPont

†SINEQUAN®

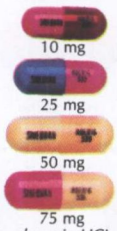

10 mg
25 mg
50 mg
75 mg
doxepin HCl
Roerig

†SPARINE®

25 mg
50 mg
100 mg
promazine HCl
Wyeth-Ayerst

†STELAZINE®

2 mg
trifluoperazine HCl
SmithKline Beecham

†STRATTERA®

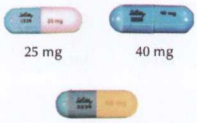

25 mg
40 mg
60 mg
atomoxetine HCL
Eli Lilly

†SURMONTIL®

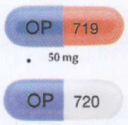

50 mg
100 mg
trimipramine maleate
Odyssey Pharmaceuticals, Inc.

†SYMBYAX®

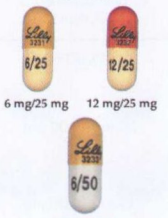

6 mg/25 mg
12 mg/25 mg
6 mg/50 mg
olanzapine and fluoxetine HCl
Eli Lilly

†SYMMETREL®

100 mg
amantadine HCl
Du Pont Multi-Source

†TARACTAN®

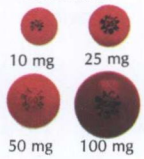

10 mg
25 mg
50 mg
100 mg
chlorprothixene
Roche

TEGRETOL®

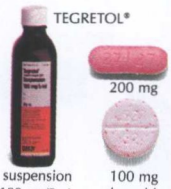

suspension
100 mg/5mL
200 mg
100 mg
chewable
carbamazepine
Basel

†THORAZINE®

25 mg
chlorpromazine HCl
SmithKline Beecham

†TOFRANIL®

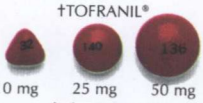

10 mg
25 mg
50 mg
imipramine HCl
Novartis

TOFRANIL-PM®

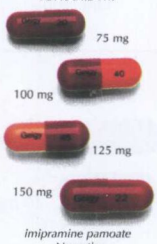

75 mg
100 mg
125 mg
150 mg
imipramine pamoate
Novartis

†TRANXENE® T-TAB®
Tablets

7.5 mg
clorazepate dipotassium
Abbott

TRIAVIL®

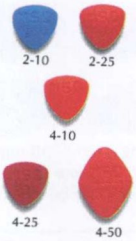

2-10
2-25
4-10
4-25
4-50
perphenazine-amitriptyline HCl
Merck & Co.

†TRILAFON®

4 mg
perphenazine
Schering

†TRILEPTAL®

150 mg
300 mg
oxcarbazepine
Novartis

†VALIUM®

2 mg
5 mg
10 mg
diazepam
Roche

†VISTARIL®

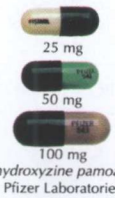

25 mg
50 mg
100 mg
hydroxyzine pamoate
Pfizer Laboratories

VIVACTIL®

5 mg
10 mg
protriptyline HCl
Odyssey Pharmaceuticals

†VYVANSE®

70 mg
lisdexamfetamine dimesylate
Shire LLC

†WELLBUTRIN®

75 mg
100 mg
bupropion HCl
Burroughs Wellcome

†WELLBUTRIN XL®

150 mg
300 mg
bupropion HCl
extended release tablets
GlaxoSmithKline

†XANAX®

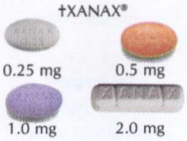

0.25 mg
0.5 mg
1.0 mg
2.0 mg
alprazolam
Upjohn

YOCON®

5.4 mg
yohimbine HCl
Palisades Pharmaceutical

ZOLOFT®

100 mg
50 mg
sertraline HCl
Roerig

†ZONEGRAN®

100 mg
zonisamide
Elan

ZYPREXA®

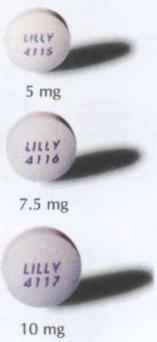

5 mg
7.5 mg
10 mg
olanzapine
Eli Lilly

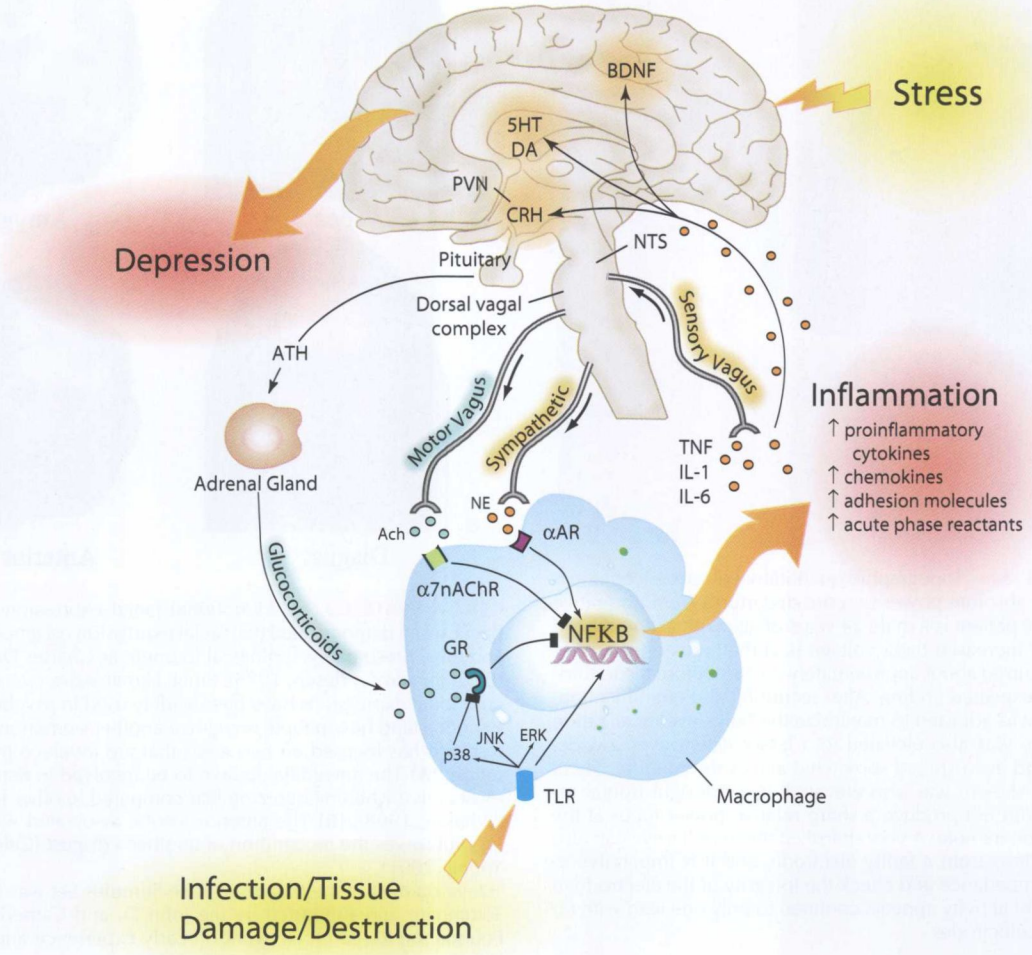

COLOR PLATE 1.13–7. Stress and bidirectional neural–immune interactions. **(a)** Activation of NF-κB through toll-like receptors (TLRs) during immune challenge leads to an inflammatory response including **(b)** the release of proinflammatory cytokines, TNF-α, IL-1, and IL-6. **(c)** These cytokines, in turn, access the brain via leaky regions in the blood–brain barrier, active transport molecules, and afferent nerve fibers (e.g., sensory vagus), which relay information through the nucleus tractus solitarius (NTS). **(d)** Once in the brain, cytokine signals participate in pathways known to be involved in the development of depression, including: (i) altered metabolism of relevant neurotransmitters such as serotonin (5HT) and dopamine (DA), (ii) activation of CRH in the paraventricular nucleus (PVN) and the subsequent production and/or release of ACTH and glucocorticoids (cortisol), and (iii) disruption of synaptic plasticity through alterations in relevant growth factors (e.g., brain-derived neurotrophic factor [BDNF]). **(e)** Exposure to environmental stressors promotes activation of inflammatory signaling (NF-κB) through increased outflow of proinflammatory sympathetic nervous system responses (release of norepinephrine [NE], which binds to the α [αAR] and β [βAR] adrenoceptors). **(f)** Stressors also induce withdrawal of inhibitory motor vagal input (release of acetylcholine [Ach], which binds to the α7 subunit of the nicotinic acetylcholine receptor [α7nACRh]). **(g)** Activation of the mitogen-activated protein kinase pathways, including p38 and Jun N-terminal kinase (JNK), inhibit the function of glucocorticoid receptors (GRs), thereby releasing NF-κB from negative regulation by glucocorticoids released as a result of the hypothalamic-pituitary-adrenal (HPA) axis in response to stress. (From *Trends in Immunology, 27,* Raison CL, Capuron L, Miller AH, Cytokines sing the blues: inflammation and pathogenesis of depression, 24–31, 2006, with permission from Elsevier.)

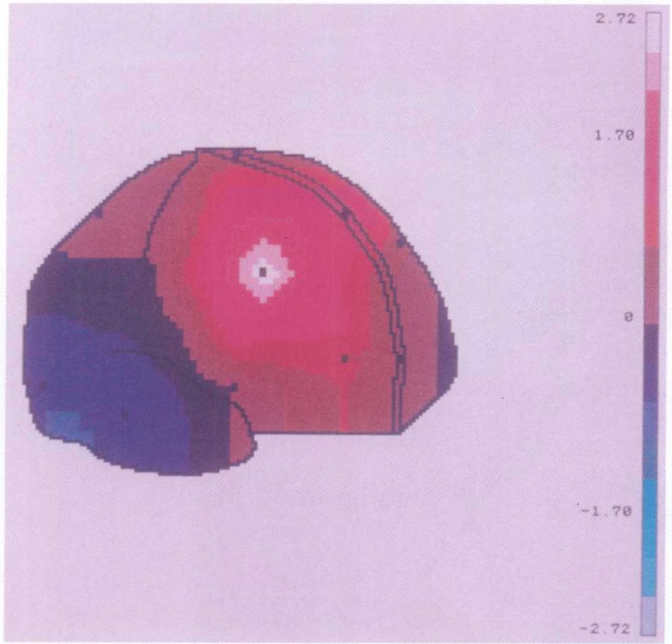

COLOR PLATE 1.15–24. Topographic quantitative electroencephalography map of theta absolute power (*z* score departures from normative database mean). The patient is a male 24 years of age with a closed head injury. The focus of increased theta voltage is at the locus of an earlier head injury that occurred about approximately 2 years before the recording. This was an unexpected finding. After recording and quantification, the color bar scale was adjusted to maximize the bull's-eye localization effect. Theta voltage was also elevated to a lesser extent over a wide, right frontal area and even spread somewhat across the midline. Theta relative power (not shown) was also elevated over the right frontal region, but mapping did not produce a sharp relative power focus at the locus of injury. Important note: A very sharply defined bull's eye can also be produced by artifact from a faulty electrode, and it is imperative to monitor electrical impedance and check the integrity of the electrode in the event that deviant activity appears confined to only one lead with no spread to adjoining electrodes.

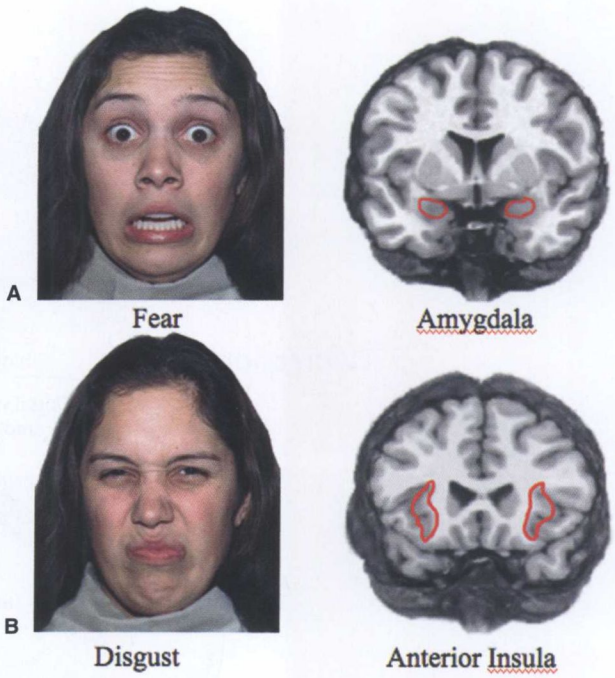

COLOR PLATE 1.22–4. Emotional facial expressions[1]. In the 1960s, Paul Ekman demonstrated that facial expressions of emotion are universal and thus, presumably, biological in origin as Charles Darwin once theorized (Ekman & Friesen, 1975). Since Ekman's discovery, photographs of emotional expressions have been widely used in psychological research to understand how people recognize another's emotions. Neuroimaging research has focused on two areas that are involved in emotion recognition: **(A)** The amygdala, known to be involved in fear conditioning, is most active when recognizing fear compared to other facial expressions (Whalen, 1998). **(B)** The anterior insula, associated with taste processing, subserves the recognition of another's disgust (Calder, Lawrence, & Young, 2001).

[1] Development of the MacBrain Face Stimulus Set was overseen by Nim Tottenham and supported by the John D. and Catherine T. MacArthur Foundation Research Network on Early Experience and Brain Development.

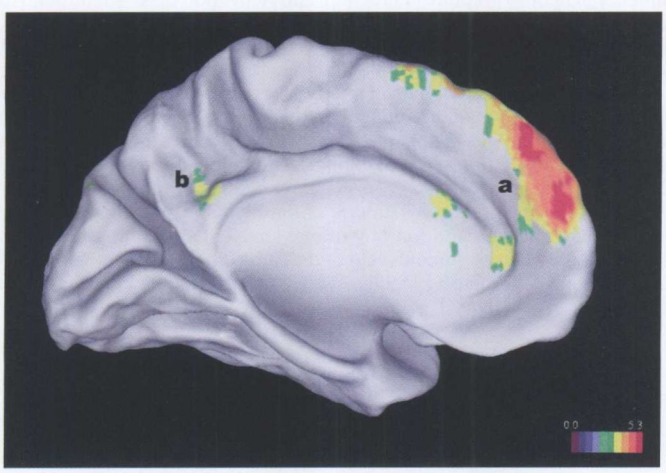

COLOR PLATE 1.23–2. Statistical activation map of the contrast between participants' judgments of their own feelings about variably evocative scenes and their judgments of whether these same scenes appear to be indoors or outdoors ($n = 24$ normal participants). Relatively greater activation is commonly seen in the dorsal medial prefrontal/paracingulate (**a**) and posterior cingulate/retrosplenial (**b**) regions in such experimental tasks, where attention to subjective states is of primary interest. Other experimental data suggest that the medial prefrontal region may be more significant for the instrumental aspects of self-reflection, while the posterior medial cortex may be more significant for experiential (including memory-related) aspects of self-reflection. These regions are also part of a network of brain regions that "deactivate" during the performance of a wide variety of demanding cognitive tasks (e.g., mental arithmetic), which has led to the suggestion that this network subserves a "default mode" of brain functioning that is self-referential (ranging from body-monitoring to reflection on an individual's past and future states). (See Gusnard DA, Akbudak E, Shulman GL, Raichle ME: Medial prefrontal cortex and self-referential mental activity: Relation to a default mode of brain function. *Proc Natl Acad Sci U S A.* 2001;98:4259.)

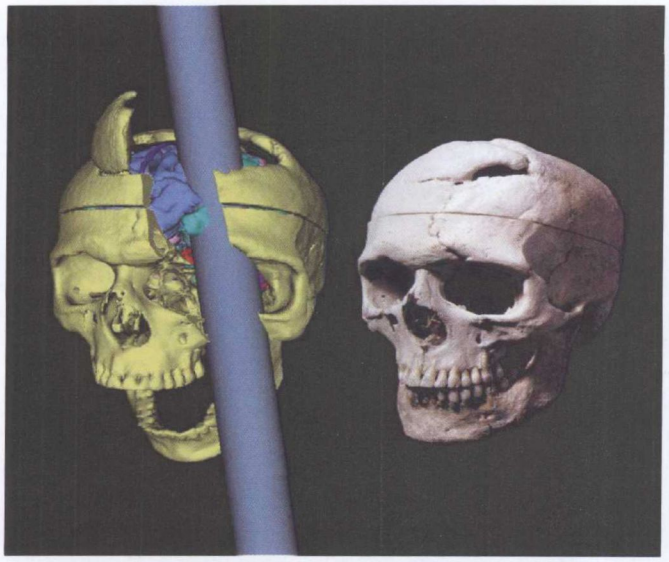

COLOR PLATE 2.5–1. Three-dimensional reconstruction of then Phineas Gage trauma showing the trajectory of the penetrating rod injuring the left orbital and ventromedial prefrontal cortices. (From Ratiu P, Talos IF: *N Engl J Med.* 2004;351:e21, with permission.) (For another picture of Phineas Gage, see Fig. 1.23–1 on p. 356.)

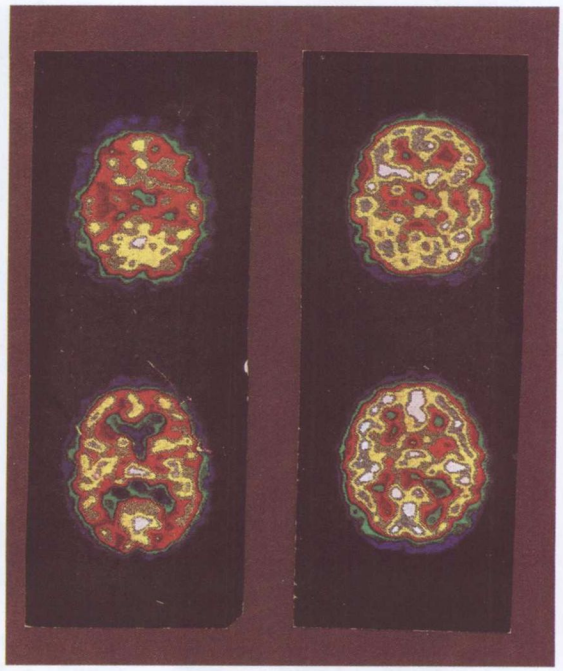

COLOR PLATE 2.9–1. Single-photon emission computed tomography (SPECT) scan demonstrating multiple areas of decreased blood flow in a Lyme patient (L) compared to a healthy control (R).

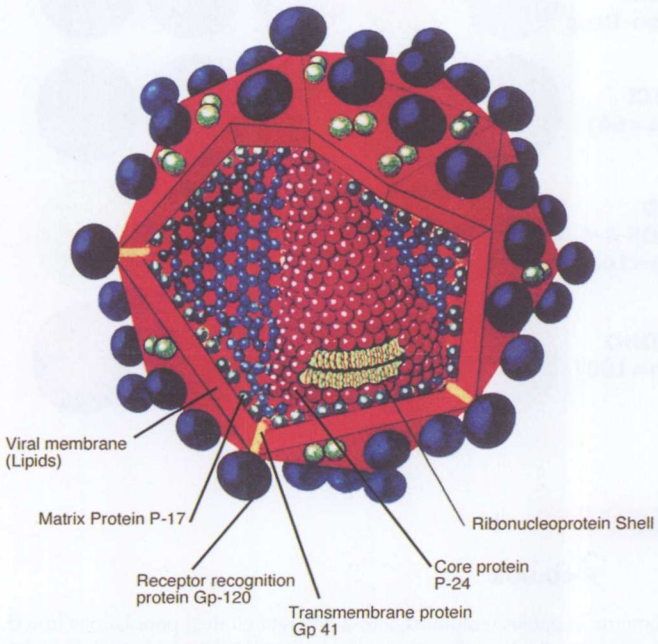

COLOR PLATE 2.8–1. Human immunodeficiency virus viral particle with its lipid envelope. (Courtesy of Milan V. Nermut, M.D., Ph.D., D.Sc.)

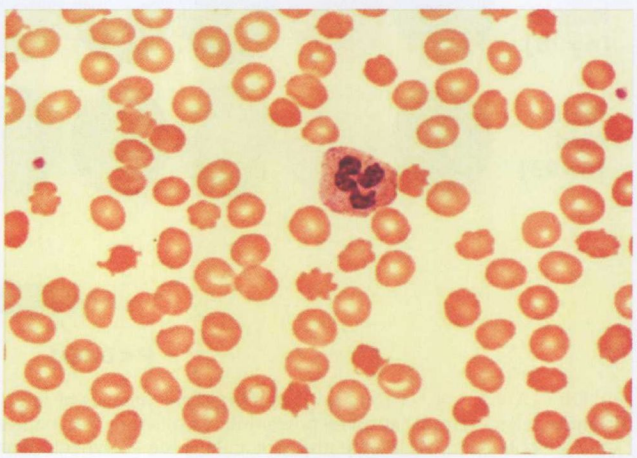

COLOR PLATE 2.14–11. A 38-year-old woman with neuroacanthocytosis who first presented with adolescent obsessive-compulsive symptoms prior to adult-onset seizures and chorea. Blood smear showing characteristic red cell acanthocytes.

COLOR PLATE 2.14–21. Reversibility in Hashimoto's encephalopathy. Single photon emission computed tomography (SPECT) showing gross global hypoperfusion in all nonoccipital regions in a 59-year-old woman with rapidly progressive cognitive impairment and myoclonus, with Mini-Mental State Examination (MMSE) score of 20 (*top*) and after significant clinical improvement 6 weeks later, when MMSE score was 27 (*bottom*). (From Forchetti CM, Katsamakis G, Garron DC: Autoimmune thyroiditis and a rapidly progressive dementia: Global hypoperfusion on SPECT scanning suggests a possible mechanism. *Neurology.* 1997;49:623, with permission.)

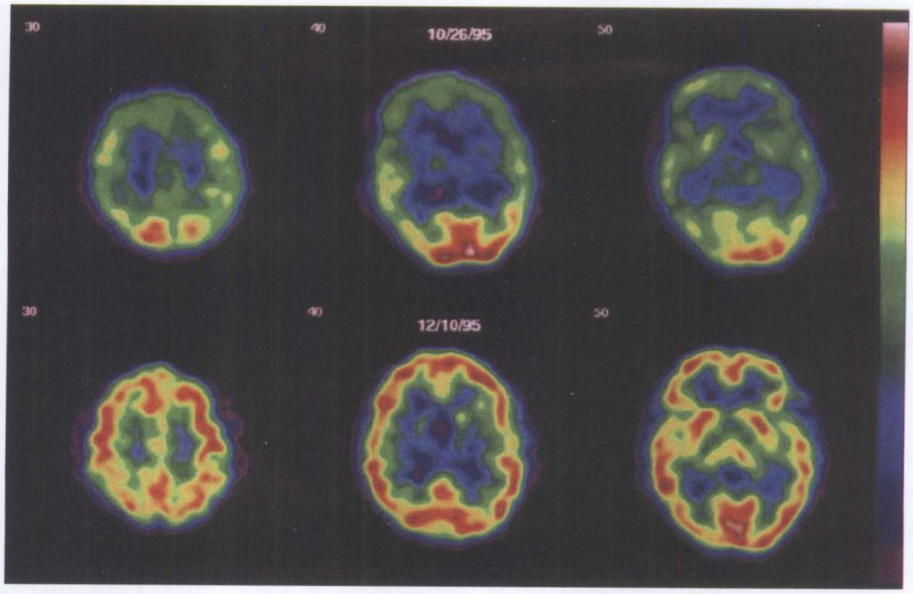

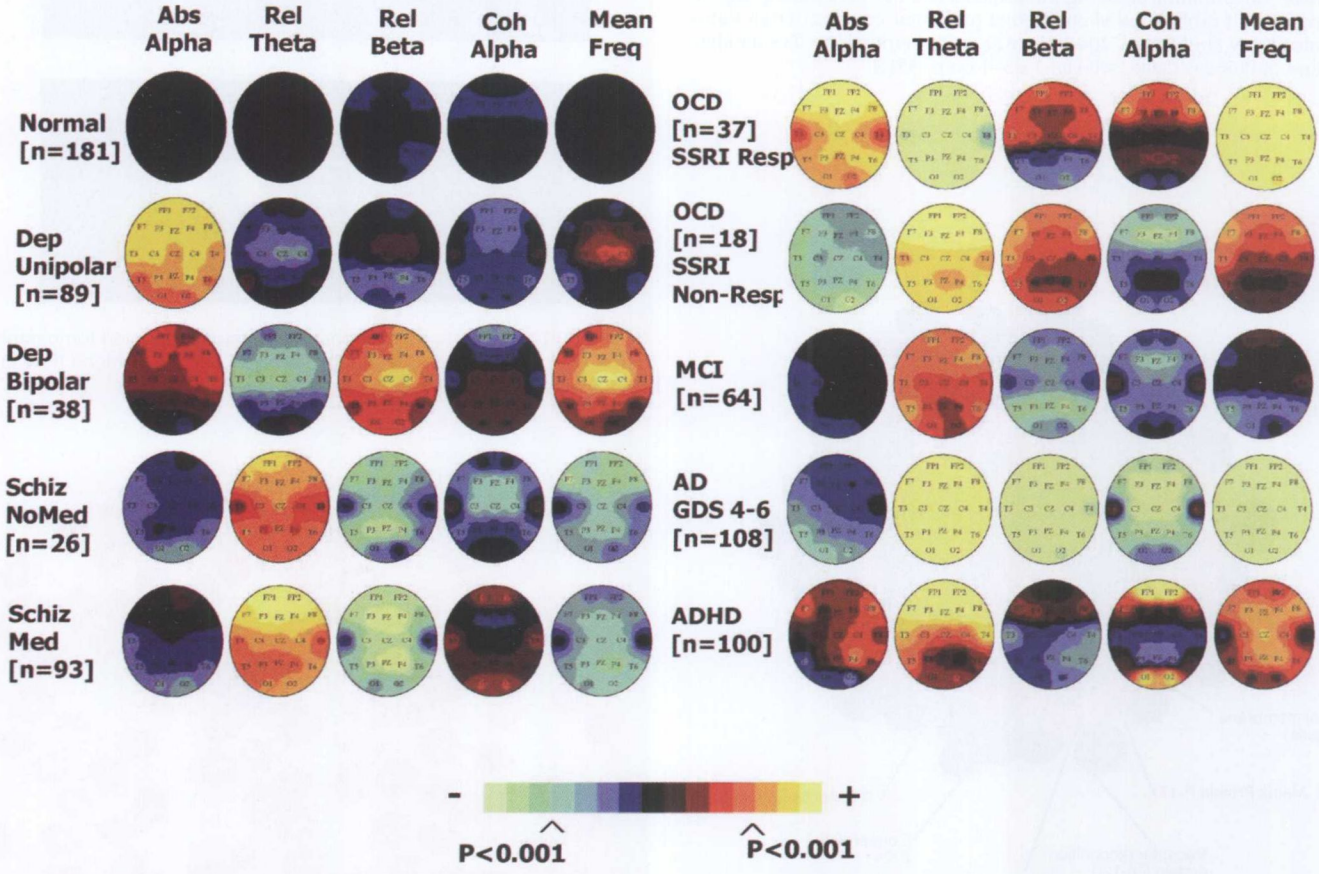

COLOR PLATE 7.9–4. Group average topographic images of selected neurometric variables (columns) across different clinical populations (rows). Columns, left to right: (1) absolute power (microvolts squared) in the alpha frequency band; (2) relative power (%) in the theta band; (3) relative power (%) in the beta band; (4) interhemispheric coherence (% synchronization) in the alpha band; and (5) mean frequency of total spectra of the EEG (Hz). (*Left*) Row 1, Normal individuals not used to construct the norms ($N = 181$); Row 2, Unipolar patients in depressed state ($N = 89$); Row 3, Bipolar patients in depressed state ($N = 38$); Row 4, Chronic schizophrenic patients, nonmedicated >3 months ($N = 26$); Row 5, Chronic schizophrenic patients, currently on medication ($N = 93$). (*Right*) Row 1, Drug-free baseline data in obsessive–compulsive disorder (OCD) patients who go on to be selective serotonin reuptake inhibitor (SSRI) responders ($N = 37$); Row 2, Drug-free baseline data in OCD patients who go on to be SSRI Non-responders ($N = 18$); Row 3, mild cognitively impaired (MCI) elderly patients with a GDS staging of 3 ($N = 64$); Row 4, Alzheimer's disease (AD), with GDS staging of 4–6, ($N = 108$); Row 5, Children with attention-deficit/hyperactivity disorder (ADHD) ($N = 100$). The color scale is proportional to the significance of the deviation from age-expected normal values, with black, no departure; blue to light green, deficits; and red to yellow, excesses. Statistical significance of entry for any group can be estimated by multiplying the value of the indicated hue on the *Z* score color bar by the square root of the group *N*.

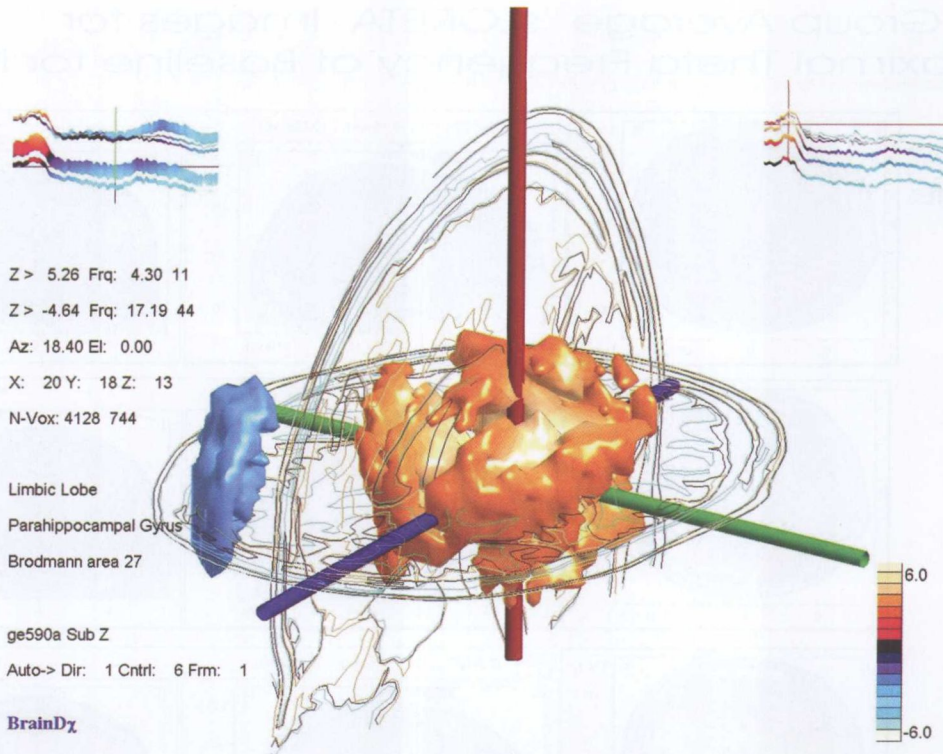

COLOR PLATE 7.9–6. Three-dimensional low-resolution electromagnetic tomographic analysis (LORETA) image of a "dissolved brain" of a patient with AD, after removal of all voxels with a *Z* score less than 3.29 ($p < .001$). The maximum theta excess (*dark red shading*, 4.3 Hz) relative to age-expected normal values is in the hippocampal and parahippocampal regions, while the frontal cortex (Brodmann area 27) reveals a minimum beta deficit (*blue*, 17 Hz).

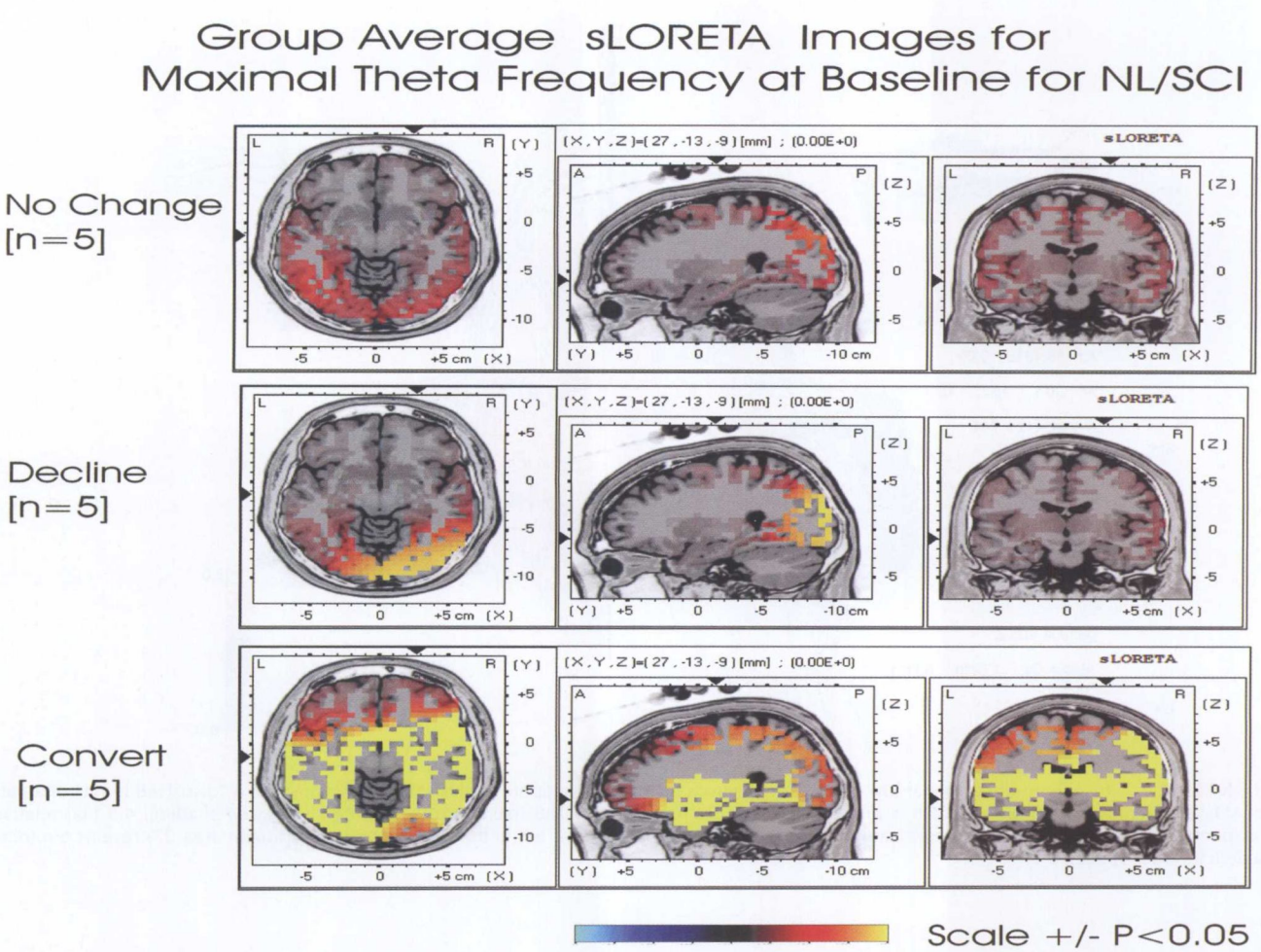

COLOR PLATE 7.9–9. Group average low-resolution electromagnetic tomographic analysis (LORETA) images ($N = 5$ in each group) of the regions displaying a maximal excess of theta activity at baseline for three different groups ($N = 5$ in each group) of elderly patients with only subjective complaints of impairment (SCI), all diagnosed as GDS 2, with no demonstrable neurocognitive deficits, who upon long-term follow-up (5 to 7 years) were found to show: Top row, no change; middle row, decline to mild cognitive impairment (MCI); bottom row, conversion to Alzheimer's disease (AD), with GDS 4–6 and substantial impairment. The images in each row, from left to right, depict transaxial, sagittal, and coronal slices automatically selected to intersect at the coordinates of the voxel that had the most deviant standard score for excessive theta activity (4.3 Hz). Each voxel is color-coded for the statistical significance of excess theta in standard scores, with hues ranging from red to yellow as significance of abnormality increases. Regions of increasing abnormalities include hippocampus, parahippocampus, and parietal-temporal cortex, as also indicated in other brain imaging methods.

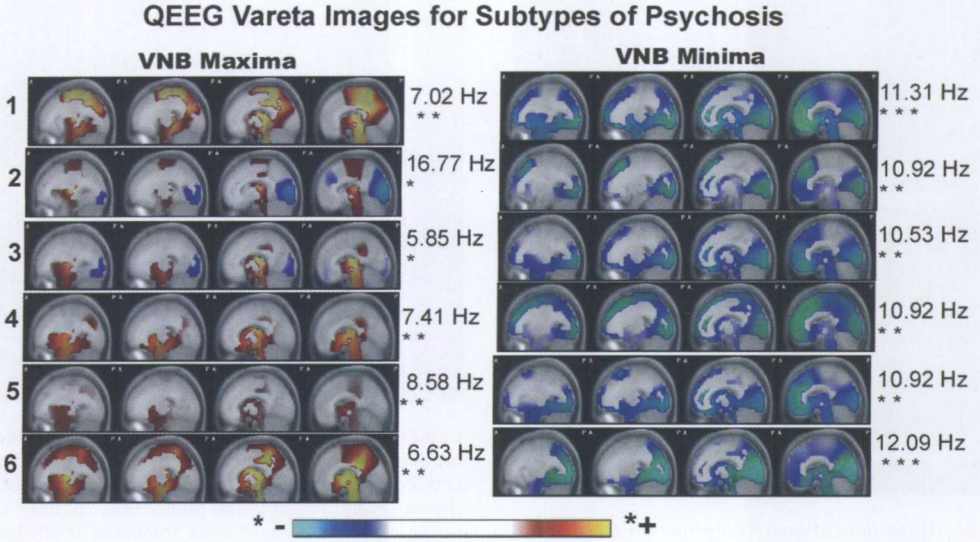

COLOR PLATE 7.9–10. From top to bottom, each row depicts group average quantitative electroencephalography (QEEG) variable resolution electromagnetic tomographic analysis (VARETA) images of selected sagittal slices from the six subtypes (1–6) of psychotic patients identified by cluster analysis of a population of 377 psychiatric patients, all of whom were psychotic. Each cluster contained patients who had received a variety of fourth revised edition of the *Diagnostic and Statistical Manual of Mental Disorders* (DSM-IV-TR)/tenth edition of the *International Statistical Classification of Diseases and Related Health Problems* (ICD-10) diagnoses, including alcoholism, depression, and chronic medicated, unmedicated, and never-medicated first-episode schizophrenia (see text). (*Left*) Sagittal slices depicting the anatomical regions that had the maximum excessive activity are shown, and (*right*) the corresponding slices with the most deficient activity, with the corresponding most deviant very narrow band (VNB) spectral frequencies of each subtype indicated at the right side of each set of slices, are shown. Note that the most deviant excessive frequencies (Hz) of the six clusters (*left*) cover a wide range, 7.0, 16.77, 5.85, 7.41, 8.58, 6.63 Hz, and were found in a diverse set of brain regions, suggesting a variety of putative upregulated neurotransmitters, while the most deficient frequencies were within a very narrow range, 11.31, 10.92, 10.53, 10.92, 10.92, 12.09 Hz, and were found in a very consistent set of brain regions, suggesting a very small set or possibly even a single downregulated neurotransmitter. The deviation from normative values of every voxel in each slice is color-coded proportional to standard scores, with the appropriate hues corresponding to the color bar that is shown below. Note that the statistical significance of the hues of each voxel can be estimated by multiplying the Z score of the corresponding value from the color bar (and the palette range is indicated for each row by: *, ± 1.0; **, ± 2.0; ***, ± 2.5) by the square root of the cluster size N, where: Clus 1, $N = 53$; Clus 2, $N = 93$; Clus 3, $N = 65$; Clus 4, $N = 24$; Clus 5, $N = 110$; Clus 6, $N = 32$. Thus, all voxels colored other than gray in these slices are extremely deviant from normative values, with a minimum $p < .001$.

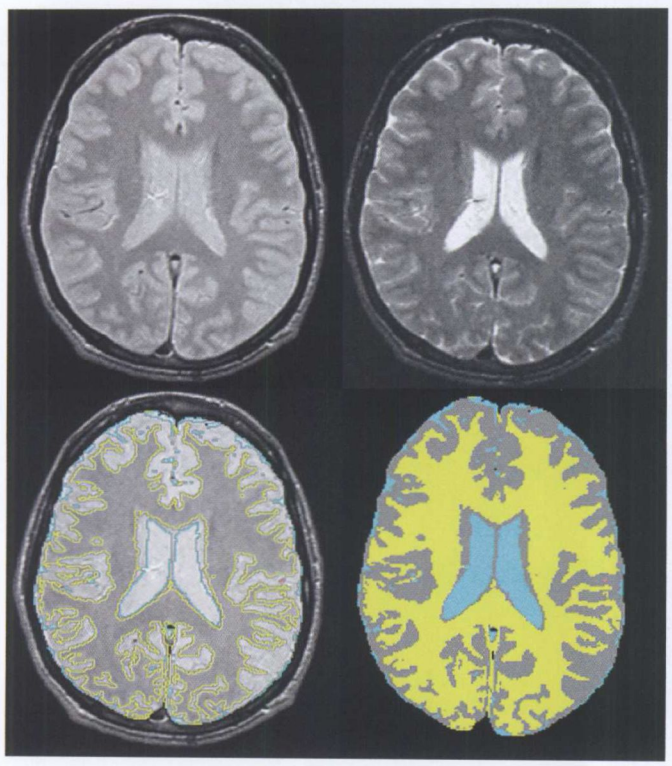

COLOR PLATE 12.7–5. Segmentation is a method whereby each voxel (volume of a pixel) in an image, or set of images, is assigned to a tissue class based on signal intensity information and neighboring voxels. On the top left is a proton density (PD) weighted image and on the top right is a T2-weighted image that shows good contrast between brain and cerebrospinal fluid (CSF). Information from both images is combined to segment the brain into gray matter (gray), white matter (yellow), and CSF (blue). (Created using three-dimensional slicer: http://www.slicer.org/.)

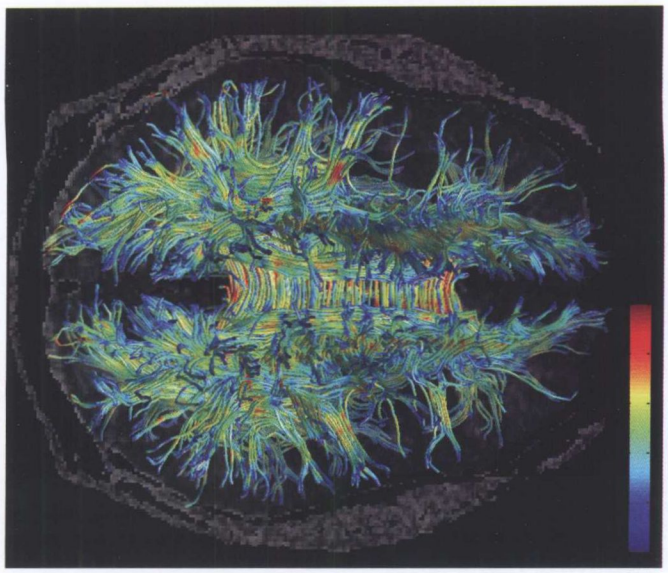

COLOR PLATE 12.7–8. Three-dimensional reconstruction based on diffusion data acquired on a 3-T General Electric scanner, Department of Radiology, Brigham and Women's Hospital, Harvard Medical School, Boston, MA. Diffusion tensor imaging (DTI) image shows major long fiber tracts of the brain. (Courtesy of Hae-Jeong Park, Ph.D., at the Laboratory of Molecular Neuroimaging, Department of Diagnostic Radiology, Yonsei University College of Medicine, Seoul, South Korea.)

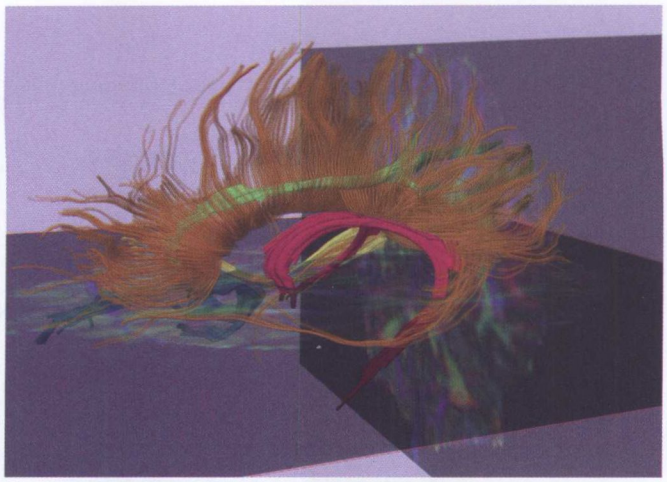

COLOR PLATE 12.7–9. Three-dimensional image reconstructed based on diffusion data acquired on a 3-T General Electric scanner, Brigham and Women's Hospital, Harvard Medical School, Boston, MA, which shows several major white matter fiber bundles identified through diffusion tensor imaging: Fornix (*magenta*), right Cingulum (*green*), right inferior longitudinal fasciculus (*yellow*), right uncinate fasciculus (*blue*), corpus callosum (*orange*). (Courtesy of Sylvain Bouix, Ph.D., Psychiatry Neuroimaging Laboratory, Department of Psychiatry, Brigham and Women's Hospital, Harvard Medical School, Boston, MA.)

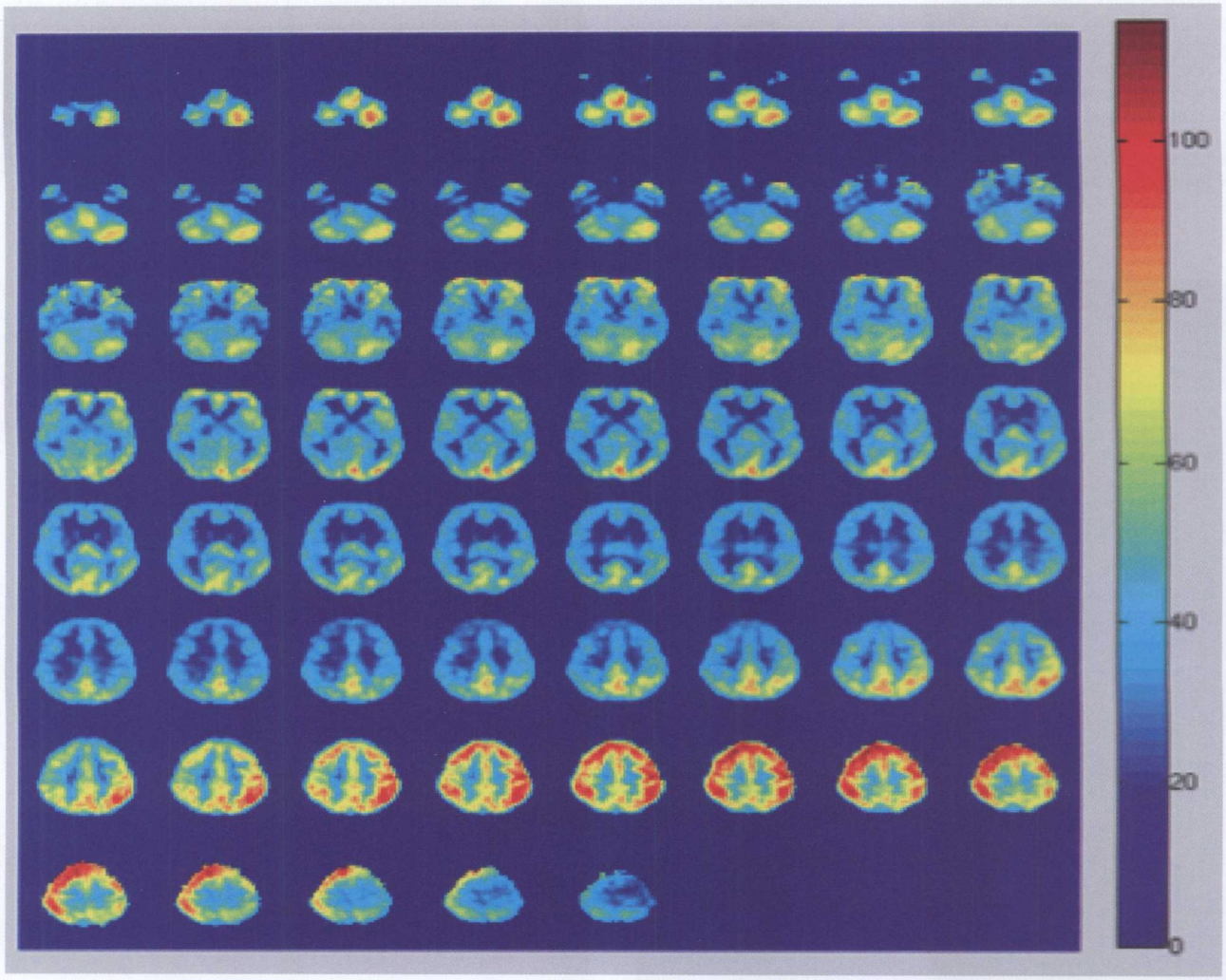

COLOR PLATE 12.8–4. Map of quantitative blood flow obtained in a healthy individual with arterial spin labeling magnetic resonance imaging.

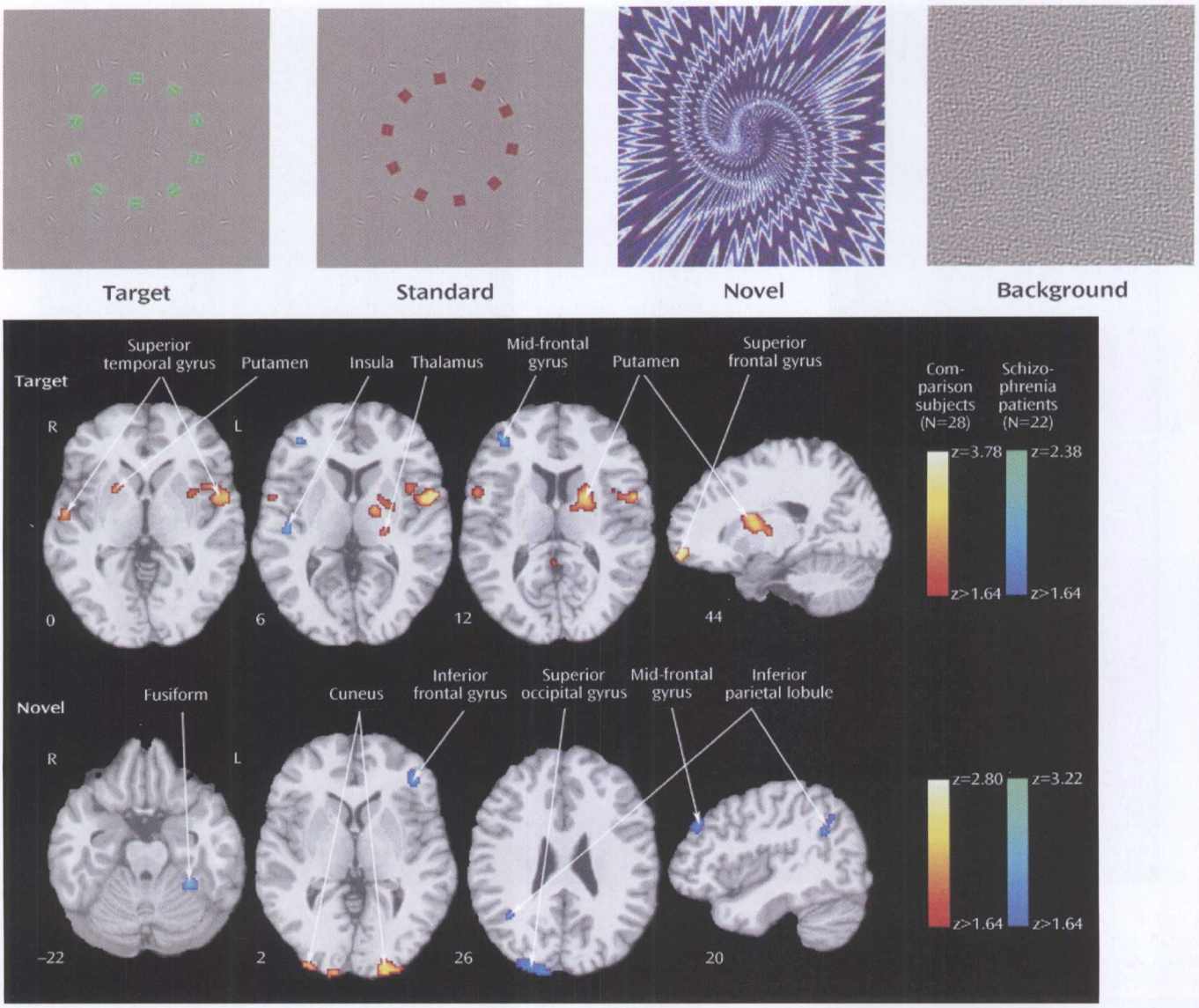

COLOR PLATE 12.8–8. Examples of stimuli used in "oddball" studies of attentional processing (*top*) and contrast images of patients with schizophrenia and comparison subjects for target and novel stimuli. Greater activation in patients is depicted by the scale on the right, whereas greater activation in comparison subjects is shown by the scale on the left. Images are in radiological convention (left hemisphere to viewer's right). (From Gur RE, Turetsky BI, Loughead J, Snyder W, Kohler C: Visual attention circuitry in schizophrenia investigated with oddball event-related functional magnetic resonance imaging. *Am J Psychiatry*. 2007;164:442, with permission.)

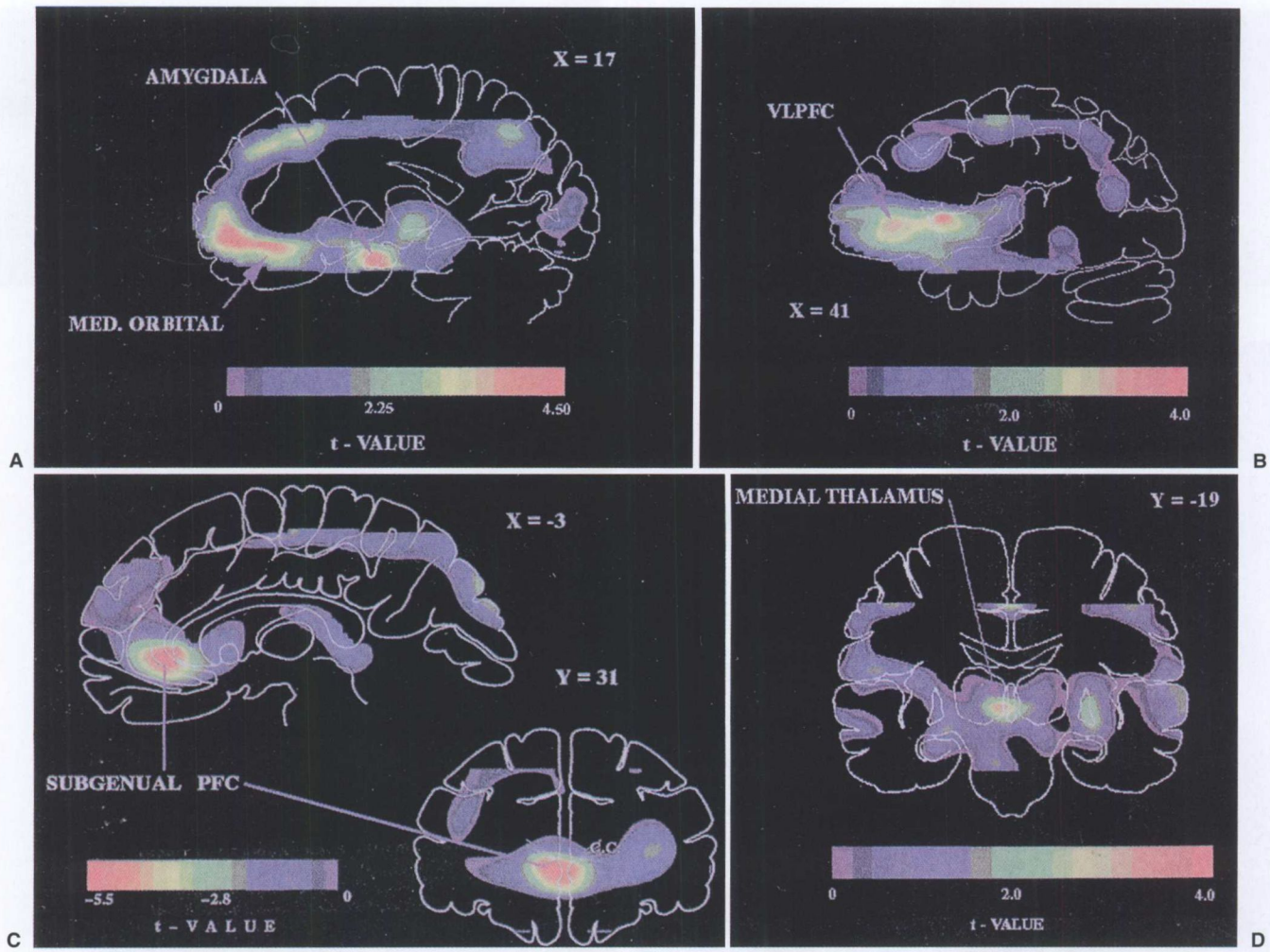

COLOR PLATE 13.4–2. Composite coronal and sagittal sections of positron emission tomography scans show areas in which cerebral glucose metabolism is decreased in depressed patients relative to matched healthy controls. PFC, prefrontal cortex; VLPFC, ventrolateral prefrontal cortex. (From Wayne Drevets, M.D.; and from *Annu Rev Med.* 2002:49 by Annual Reviews, http://annualreviews.org, with permission.)